# Pre-stress and cortical stiffness affect fluidity of living cells

Andrea Mareike Cordes[1], Hannes Witt[2], Aina Gallemí-Pérez[2], Bastian Rouven Brückner[1], Florian Grimm[1,3], Marco Tarantola[2,4*], and Andreas Janshoff[1*]

[1]*Institute of Physical Chemistry, Georg-August-Universität Göttingen, 37077 Göttingen, Germany*

[2]*Max Planck Institute for Dynamics and Self-Organization, 37077 Göttingen, Germany*

[3]*Abberior GmbH, 37077 Göttingen, Germany and*

[4]*Institute for Dynamics of Complex Systems, Georg-August-Universität Göttingen, 37077 Göttingen, Germany*

## Abstract

Shape, dynamics and viscoelastic properties of eukaryotic cells are largely governed by a thin reversibly cross-linked actomyosin cortex located directly beneath the plasma membrane. We obtain time-dependent rheological responses of weakly adhered mesenchymal cells (fibroblasts) and epithelial cells (MDCK II) from parallel-plate compression and force relaxation experiments. We introduce an analytical expression for the compression and force relaxation based on the elastic-viscoelastic correspondence principle by treating the cell as a closed liquid-filled shell and assuming a power law to describe the change of surface area during deformation. This approach gives access to pre-stress, area compressibility modulus and the power law (fluidity) coefficient, which we modulate by interfering with myosin activity. We find that the fluidity of cells decreases with increasing intrinsic pre-stress as shown for isolated actin networks subject to external stress.

PACS numbers: 87.15.La, 82.35.Lr, 87.16.Ka, 87.16.Ln

Many cellular processes such as adhesion, motility, growth, and development are tightly associated with the mechanical properties of cells and their environment [1–3]. Vitality and fate of cells are often directly inferred from their elastic properties [4–7]. In search for effective and standardized mechanical phenotyping of living cells, a number of tools have been developed that permit precise measurements and even high-throughput assays based on optical stretchers or microfluidic devices are available that allow to analyze many thousands of cells in suspension in a very short time [7]. It is indisputable that the mechanical response of cells to external deformation is predominately caused by the cellular cortex [8, 9]. The cortex forms a composite shell consisting of a compliant but contractile actin mesh with a large number of actin binding proteins coupled to an almost inextensible lipid membrane [10, 11]. The thin actin cortex can be contracted by the action of motor proteins such as myosin II resulting in a measurable pre-stress that provides resistance against deformation at low strain for adherent cells [8, 12]. As first pointed out by Fredberg, Fabry and coworkers, rheological parameters of compliant cells such as the complex shear modulus generally obey a power law dependency $G^* \propto \omega^{-\beta}$ over multiple decades in frequency $\omega$, reflecting an intricate energy landscape provided by a reversibly and actively remodeled cross-linked cytoskeleton [13, 14]. The dimensionless power law coefficient $\beta$ characterizes the degree of fluidity and energy dissipation upon deformation, where $\beta = 0$ represents an ideal elastic solid and $\beta = 1$ a Newtonian liquid. Values obtained for the power law coefficient of living cells are usually independent of cell type and range between 0.2 – 0.4 for adherent cells [4, 13] and 0.3 – 0.6 for cells in suspension [15, 16]. However, the description of rheological spectra or associated response functions (creep or relaxation) almost exclusively relies on models based on contact mechanics. As a consequence, the current models treat the cells as a semi-infinite continuum and neglect their composite nature, shell-like geometry, fluid core and the existence of pre-stress [4, 13]. The challenge lies in closing the gap between the rheological properties found for living cells and those of artificial actin cortices. A large leap forward was recently made when Mulla *et al.* could show for reversibly linked artificial actin networks that transient cross-linking combined with internal stress can explain the low power law coefficients observed for cells [17]. Our goal is to obtain fundamental insight into the universal impact of internal stress on the viscoelastic properties of cells. As a consequence, a viscoelastic model is required that permits to relate pre-stress of cells to fluidity from deformation-relaxation experiments. Concretely, we devise an analytical viscoelastic model

of the cortex based on power law rheology that permits to describe force compression-relaxation curves recorded at different velocities and forces over the entire experimental time scale. We use parallel-plate-like compression and relaxation of cells with an atomic force microscope and took measures to minimize adhesion of cells that might compromise their spherical shape (Fig. 1A) [18]. Drugs like blebbistatin [19] and calyculin A [20] were administrated to arrest and boost myosin activity, respectively, allowing us to alter the intrinsic pre-stress in a predictable fashion.

In our model we consider the thin cortex as a two-dimensional continuous material with negligible bending stiffness and zero area shear modulus [21–23]. We refer to this model as the *viscoelastic Evans* model throughout the text due to his seminal and initial work on cortex mechanics [21]. Viscoelasticity of the 2D area compressibility modulus is assumed to follow a power law. As demonstrated previously, the experimental setup ensures small curvature of the cell cortex therefore permitting to neglect bending contributions to the Hamiltonian [18, 24, 25]. Minimizing free energy assuming constant volume leads to minimal surfaces of constant curvature with the force balance $f$ at the equatorial radius (Fig. 1B):

$$f = \frac{2\pi R_0 R_\mathrm{i}}{R_0^2 - R_\mathrm{i}^2}\left(T_0 + K_\mathrm{A}\alpha\right) \tag{1}$$

with $R_0$ the equatorial radius, $R_\mathrm{i}$ the contact radius, $\alpha = \frac{\Delta A}{A_0}$ the relative area change, $T_0$ the pre-stress and $K_\mathrm{A}$ the area compressibility modulus of the cortex. It is straightforward to cast the model into non-dimensional form that permits to write eq. (1) as $g\left(\xi\right) = \frac{f}{R_\mathrm{c} T}$, with $\xi = z/R_\mathrm{c}$ (Fig. 1B). $R_\mathrm{c}$ is the initial radius of the cell in suspension and $T$ denotes the overall homogeneous tension. Hence, $g(\xi)$ and $\alpha(\xi)$ are generic functions that only need to be computed once. Both functions can easily be approximated by polynomials $g(\xi) \approx \sum_{i=1}^{n} c_\mathrm{i}\xi^i$ and $\alpha(\xi) \approx \sum_{i=1}^{n} d_\mathrm{i}\xi^i$ permitting to obtain an analytical solution of the corresponding elastic-viscoelastic problem (usually $n = 3$ is sufficient to reach an accurate result, see supplementary information, SI). The general hereditary integrals for the restoring force during compression $f_\mathrm{comp}$ ($0 < t < t_\mathrm{m}$, eq. (2)) and relaxation $f_\mathrm{rel}$ ($t > t_\mathrm{m}$, eq. (3)) read [26]:

$$f_\mathrm{comp} = g(\xi) R_\mathrm{c}\left(T_0 + \int_0^t K_\mathrm{A}(t-\tau)\frac{\partial\alpha(\tau)}{\partial\tau}\mathrm{d}\tau\right) \tag{2}$$

$$f_{\mathrm{rel}} = g(\xi) R_{\mathrm{c}} \left( T_0 + \int_0^{t_{\mathrm{m}}} K_{\mathrm{A}}(t-\tau) \frac{\partial \alpha(\tau)}{\partial \tau} \mathrm{d}\tau + \int_{t_{\mathrm{m}}}^{t} K_{\mathrm{A}}(t-\tau) \frac{\partial \alpha}{\partial \tau} \mathrm{d}\tau \right) \tag{3}$$

Here we use $\xi \approx \frac{v_0 t}{R_{\mathrm{c}}}$ for compression with the constant velocity $v_0$, and $\frac{\partial \alpha}{\partial t} = 0$ for relaxation. Hence, the second integral of eq. (3) vanishes naturally. Assuming a power-law behavior of $K_{\mathrm{A}} = K_{\mathrm{A0}}(t/t_0)^{-\beta}$ with the timescaling parameter $t_0$, integration of eq. (2) and (3) is straightforward (see SI). Because $K_{\mathrm{A0}}$ and $t_0$ are not independent due to the scaling invariance of the power law, $t_0$ can be chosen arbitrarily and is usually set to 1 s [14]. Therefore, the scaling parameter $K_{\mathrm{A0}}$ might deviate from the area compressibility modulus of the cortex obtained from purely elastic models.

In contrast to the proposed Evans model, Hertzian contact mechanics describes the cell as an continuous sphere in contact with a plane (see SI).

The model brings us into the position to answer the question whether power law rheology is indeed sufficient to explain force relaxation over the entire experimental timescale regardless of compression speed and to resolve some of the crucial discrepancies with rheology of artificial model systems. Therefore, it was used to analyze atomic force microscopy compression-relaxation experiments on fibroblasts (3T3) representative of mesenchymal cell types and MDCK II cells as a typical epithelial phenotype. Fig. 1B shows the actin mesh of a weakly adhered MDCK II cell imaged by STED microscopy exhibiting a thickness of merely 100 – 200 nm, hence justifying neglecting bending contributions to the Hamiltonian. Tipless cantilevers with nominal spring constants of 0.01 N/m were used to compress weakly adhering cells in a parallel-plate like fashion (Fig. 1C). We used constant approach and retraction velocities between 0.5 – 20 µm/s and a relaxation time of several seconds as indicated. Since fibroblasts strongly adhere and spread to surfaces directly after seeding, we minimized their initial adhesion by using RGD peptides or PEGylated surfaces to abolish cellular adhesion. Blebbistatin or calyculin A were added to cell medium shortly before cell seeding, where applicable. Detailed description of the experimental methods can be found in the SI.

Fig. 1D shows a typical compression-relaxation experiment with a single fibroblast. It is divided into the compression phase (i) during which the cell is loaded at constant velocity until the yield force is reached at $t_{\mathrm{m}}$ and (ii) subsequent force relaxation at constant distance

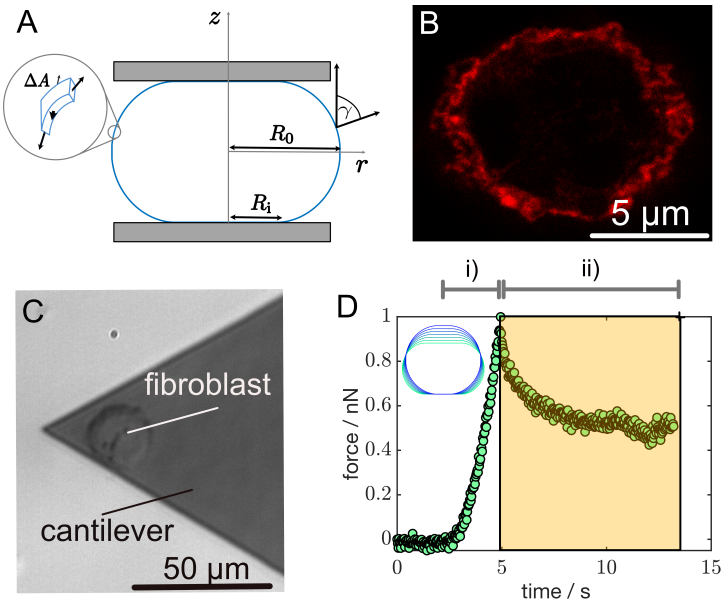


FIG. 1. A) Parametrization and shape of a cell between two parallel plates. $\gamma$ is the angle at which the normal at any point on the surface meets the vertical axis. B) Fluorescence microscopy image (STED) of a cellular cortex (red: actin) of a MDCK II cell (projection). C) Optical micrograph (bright field) showing a clamped fibroblast between a tipless cantilever and the substrate. D) Typical compression (i) at $v_0 = 0.5\,\mu$m followed by force relaxation (ii) of the fibroblast shown in (C). The inset shows the shape of the cell for various discrete $\xi$ values.

between the plates. The full curve from the contact to the end of the relaxation curve was modeled with eqs. (2,3) by adapting the three fitting parameters, cortical tension $T_0$, area compressibility modulus $K_{\mathrm{A0}}$ and the power law coefficient $\beta$ (see SI). For precise scaling, the size of each cell ($R_{\mathrm{c}}$) was measured by phase contrast microscopy prior to compression (Fig. 1C).

Before applying the model to experimental data, we want to examine the impact of the three parameters $T_0$, $K_{\mathrm{A0}}$, and $\beta$ (Fig. 2A). It becomes immediately clear, that the curve shape agrees qualitatively with Fig. 1D. While an increase in cortical tension increases the slope of the compression curve it only adds an offset to the relaxation part (A1). Increasing the area compressibility modulus influences the compression part at larger strain and also the relaxation by increasing the amount of dissipated energy (A2). Increasing $\beta$ results in a larger slope during compression and a quicker drop of the yield force at relaxation (A3). Fig. 2B shows representative fits of eqs. (2,3) to compression-relaxation curves of

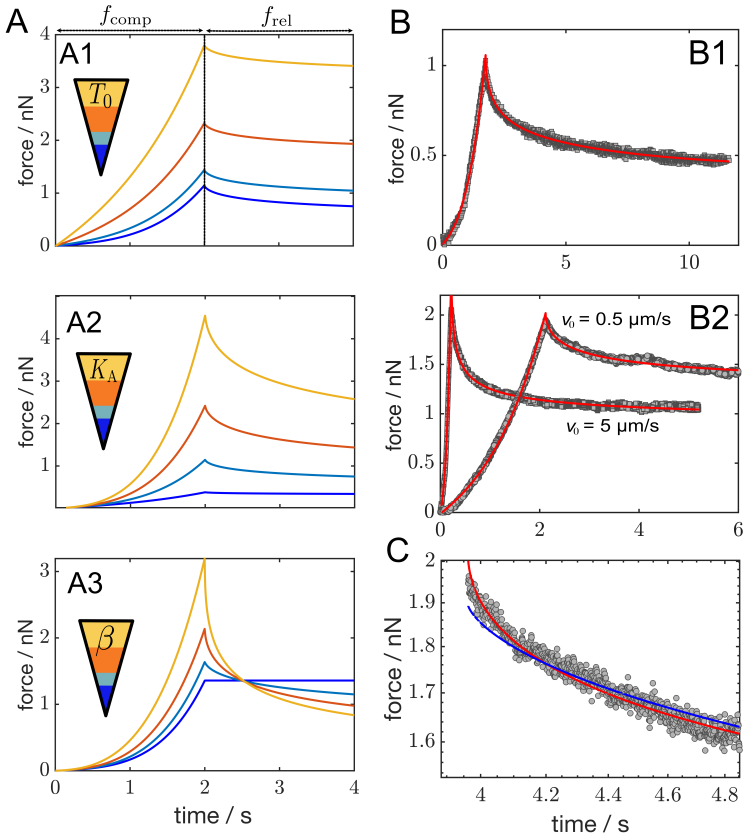


FIG. 2. A) Computed compression-relaxation curves for varying pre-stress $T_0$ (0.1, 0.2, 0.5, 1 mN/m) ($K_A$ = 0.1 N/m, $\beta$ = 0.3) (A1), area compressibility modules $K_{A0}$ (0.01, 0.1, 0.25, 0.5 N/m) ($T_0$ = 0.1 mN/m, $\beta$ = 0.3) (A2) and power law coefficients $\beta$ (0, 0.2, 0.4, 0.6) ($K_{A0}$ = 0.2 N/m, $T_0$ = 0.05 mN/m) (A3). B) Compression-relaxation curves of fibroblasts (B1) and MDCK II cells (B2) and the corresponding fits (red lines) according to eqs. (2,3). Fitting parameters for the fibroblast loaded with $v_0$ = 0.5 µm/s and $R_c$ = 7.8 µm are $T_0$ = 0.36 mN/m, $K_{A0}$ = 0.9 N/m, $\beta$ = 0.42 (B1). B2) Compression velocity does not significantly change the fitting results. Fitting parameters for MDCK II cells are $T_0$ = 0.83 mN/m, $K_{A0}$ = 0.39 N/m, $\beta$ = 0.42 for the cell compressed with 0.5 µm/s and $T_0$ = 0.57 mN/m, $K_{A0}$ = 0.24 N/m, $\beta$ = 0.43 for the same cell compressed at 5 µm/s. C) Force relaxation of a MDCK II cell after compression (0.5 µm/s) as a function of time. The fitted Evans model (red line, $\beta$ = 0.3) is compared to the fitted viscoelastic Hertz model (blue curve, $\beta$ = 0.2).

fibroblasts loaded with 0.5 µm/s (B1) and MDCK II cells loaded with 0.5 µm/s and 5 µm/s, respectively (B2). The viscoelastic Evans model fits the data for both cell types very well and also describes the curves over a large loading rate regime (0.5 – 20 µm/s, see SI). Since

hydrodynamic drag in the onset of the compression curve is only negligible at low approach speed subsequent experiments were carried out predominately at low speed ($\leq 1$ µm/s). Describing the force relaxation after compression of the cell with the viscoelastic Hertz model (eq. 4, Fig. 2C (blue line), Fig. S4) falls short at describing the initial relaxation after compression compared to the Evans model (red line). As a consequence, $\beta$ values obtained from viscoelastic Hertz mechanics are systematically smaller than those provided by the Evans model (Fig. S4B). Chadwick and coworkers proposed a poroelastic behavior of the cells (MDCK II) that was necessary to describe the initial relaxation response after fast loading [27]. Here, we show that this initial drop is well captured by simple power law rheology but requires treatment of the actomyosin cortex as a pre-stressed shell as in the proposed Evans model. Cells with very low cortical tension can be modeled by the viscoelastic Hertz model and the Evans model both providing almost identical power law coefficients (Fig. S5D).

The outcome of the fitting procedure, i.e., pre-stress $T_0$, area compressibility modulus $K_{\mathrm{A0}}$, and power law coefficient $\beta$, for fibroblasts, MDCK II cells and MDCK II cells treated with either blebbistatin or calyculin A are provided in Fig. S5A-C. Interestingly, in this early state of adhesion/development of the cells, fibroblasts and MDCK II cells display nearly identical mechanical properties stressing the universal viscoelastic features of cortices in mammalian cells. Switching off myosin activity by adding blebbistatin to weakly adhering MDCK II cells has substantial impact on the power law coefficient. An increase in $\beta$ is indicative of cortex fluidization, which we attribute to a loss of transient crosslinks otherwise provided by myosin bundles. In contrast, addition of calyculin A, which is a potent phosphatase inhibitor that increases myosin II activity results in larger cortical tension $T_0$ and slightly reduced fluidity (see SI). Generally, we find that cells with stiffer cortices display a smaller power law exponent (Fig. 3). $\beta$ decreases logarithmically with $K_{\mathrm{A0}}$ (Fig. 3A, Fig. S5E). The same has also been predicted by Gardel *et al.* [28] for the differential modulus and Kollmannsberger *et al.* [29] for the compliance of various cell types. Note that the compliance $J(t)$ is inversely proportional to the Young's modulus $E(t) = 1/J(t) = K_{\mathrm{A}}(t)/d$, with $d$ the cortex thickness.

Importantly, the model also permits to correlate internal pre-stress with fluidity. We found that an increase in internal stress due to higher myosin activity is accompanied by a reduction of the power law coefficient (Fig. 3B) suggesting that cells with a stiffer, more

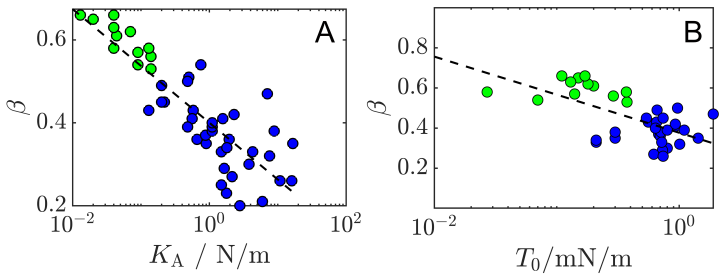


FIG. 3. Power law coefficient $\beta$ of MDCK II cells as a function of area compressibility modulus $K_{A0}$ (A) and pre-stress $T_0$ (B) for MDCK II cells under normal culture conditions (blue) and arresting myosin motors with blebbistatin (green). Dotted lines are logarithmic fits to the data.

contractile cortex are also less fluid. Recently, Mulla *et al.* found that artificial reversibly cross-linked actin networks show a decrease of $\beta$ with increasing stress [17] suggesting that the glassy dynamics of the cortex are a natural consequence of transient cross-links combined with intrinsic pre-stress. Here, we can confirm that the source of the pre-stress responsible for low $\beta$ values of the cortex of living cells are indeed myosin motors. In the absence of motor activity and therefore low pre-stress $T_0$, $\beta$ peaks around $\approx 0.5 - 0.6$ as theoretically expected for reversibly cross-linked actin filaments [17] reflecting the broad spectrum of relaxation times from the unbinding and rebinding of various crosslinkers. However, at larger pre-stress the network indeed solidifies as predicted by Koenderink and coworkers [17].

In conclusion, we found that a viscoelastic shell model is capable of describing cell compression and relaxation experiments in a consistent manner over the entire time scale. Epithelial cells show a decrease in fluidity with increasing pre-stress thereby closing the gap between rheological experiments of artificial actin networks and cortices of living cells.

The work was financially supported by the Deutsche Forschungsgemeinschaft (SFB937, A08) and the VW foundation ('Living Foams').

* ajansho@gwdg.de; mtarant@gwdg.de

[1] B. G. Godard and C.-P. Heisenberg, Curr. Op. Cell Biol. **60**, 114 (2019).

[2] J. R. Lange and B. Fabry, Exp. Cell Res. **319**, 2418 (2013).

[3] D. A. Fletcher and R. D. Mullins, Nature **463**, 485 (2010).

[4] J. Rother, H. Noding, I. Mey, and A. Janshoff, Open Biol. **4**, 140046 (2014).

[5] J. R. Staunton, B. L. Doss, S. Lindsay, and R. Ros, Sci. Rep. **6** (2016), 10.1038/srep19686.

[6] P. D. Garcia and R. Garcia, Nanoscale **10**, 19799 (2018).

[7] P.-H. Wu, D. R.-B. Aroush, A. Asnacios, W.-C. Chen, M. E. Dokukin, B. L. Doss, P. Durand-Smet, A. Ekpenyong, J. Guck, N. V. Guz, P. A. Janmey, J. S. H. Lee, N. M. Moore, A. Ott, Y.-C. Poh, R. Ros, M. Sander, I. Sokolov, J. R. Staunton, N. Wang, G. Whyte, and D. Wirtz, Nat. Meth. **15**, 491 (2018).

[8] P. Chugh, A. G. Clark, M. B. Smith, D. A. D. Cassani, K. Dierkes, A. Ragab, P. P. Roux, G. Charras, G. Salbreux, and E. K. Paluch, Nat. Cell Biol. **19**, 689 (2017).

[9] M. P. Stewart, J. Helenius, Y. Toyoda, S. P. Ramanathan, D. J. Muller, and A. A. Hyman, Nature **469**, 226 (2011).

[10] P. Chugh and E. K. Paluch, J. Cell Sci. **131**, jcs186254 (2018).

[11] R. G. Fehon, A. I. McClatchey, and A. Bretscher, Nat. Rev. Mol. Cell Biol. **11**, 276 (2010).

[12] G. Salbreux, G. Charras, and E. Paluch, Trends Cell Biol. **22**, 536 (2012).

[13] B. Fabry, G. N. Maksym, J. P. Butler, M. Glogauer, D. Navajas, and J. J. Fredberg, Phys. Rev. Lett. **87**, 148102 (2001).

[14] P. Kollmannsberger and B. Fabry, Ann. Rev. Mater. Res. **41**, 75 (2011).

[15] J. M. Maloney, E. Lehnhardt, A. F. Long, and K. J. V. Vliet, Biophys. J. **105**, 1767 (2013).

[16] C. J. Chan, A. E. Ekpenyong, S. Golfier, W. Li, K. J. Chalut, O. Otto, J. Elgeti, J. Guck, and F. Lautenschläger, Biophys. J. **108**, 1856 (2015).

[17] Y. Mulla, F. C. MacKintosh, and G. H. Koenderink, Phys. Rev. Lett. **122**, 218102 (2019).

[18] E. Schäfer, T.-T. Kliesch, and A. Janshoff, Langmuir **29**, 10463 (2013).

[19] K. A. Beningo, K. Hamao, M. Dembo, Y. li Wang, and H. Hosoya, Arch. Biochem. Biophys. **456**, 224 (2006).

[20] L. Chartier, L. L. Rankin, R. E. Allen, Y. Kato, N. Fusetani, H. Karaki, S. Watabe, and D. J. Hartshorne, Cell Motil. Cytoskeleton **18**, 26 (1991).

[21] E. Evans, R. Waugh, and L. Melnik, Biophys. J. **16**, 585 (1976).

[22] E. A. Evans and R. Skalak, *Mechanics and Thermodynamics of Biomembranes* (CRC Press, 2018).

[23] S. Sen, S. Subramanian, and D. E. Discher, Biophys. J. **89**, 3203 (2005).

[24] E. Fischer-Friedrich, Y. Toyoda, C. J. Cattin, D. J. Müller, A. A. Hyman, and F. Jülicher, Biophys. J. **111**, 589 (2016).

[25] N. Kamprad, H. Witt, M. Schröder, C. T. Kreis, O. Bäumchen, A. Janshoff, and M. Tarantola, Nanoscale **10**, 22504 (2018).

[26] R. Christensen, *Theory of Viscoelasticity* (Elsevier, 1982).

[27] E. Moeendarbary, L. Valon, M. Fritzsche, A. R. Harris, D. A. Moulding, A. J. Thrasher, E. Stride, L. Mahadevan, and G. T. Charras, Nat. Mater. **12**, 253 (2013).

[28] M. L. Gardel, F. Nakamura, J. Hartwig, J. C. Crocker, T. P. Stossel, and D. A. Weitz, Phys. Rev. Lett. **96**, 088102 (2006).

[29] P. Kollmannsberger, C. T. Mierke, and B. Fabry, Soft Matter **7**, 3127 (2011).